Journal of Biomedical Optics 8(1), 63–69 (January 2003)

Blood pO_2 and blood flow at the optic disc

Stéphane R. Chamot
Stephen D. Cranstoun
Benno L. Petrig
Institut de Recherche en Ophtalmologie
Grand Champsec 64
CP 4168, 1950 Sion 4
Switzerland

Constantin J. Pournaras
Clinique d'Ophtalmologie
Rue A. Jentzer 22
1211 Geneva 14
Switzerland

Charles E. Riva
Institut de Recherche en Ophtalmologie
Grand Champsec 64
CP 4168, 1950 Sicon 4
Switzerland
and
Université de Lausanne
Faculté de Médecine
1000 Lausanne
Switzerland

Abstract. A fundus camera-based phosphorometer to noninvasively and quasicontinuously measure the blood partial pressure of oxygen ($pO_{2,blood}$) in the microvasculature of the pig optic nerve using the principle of the phosphorescence quenching by O_2 is described. A porphyrin dye is injected into the venous circulation and the decay of its phosphorescence emission is detected locally in the eye, after excitation with a flash of light. Combined with blood flow measurements by means of a laser Doppler flowmeter mounted on the phosphorometer, we demonstrate the capability of the instrument to determine the time course of optic nerve blood flow and $pO_{2,blood}$ in response to various physiological stimuli, such as hyperoxia and hypercapnia. This instrument appears to be a useful tool for the investigation of the oxygenation of the optic nerve. © *2003 Society of Photo-Optical Instrumentation Engineers.* [DOI: 10.1117/1.1527935]

Keywords: ophthalmology; noninvasive measurements; phosphorescence; quenching; oxygen; blood flow; optic nerve.

Paper JBO 01084 received Dec. 12, 2001; revised manuscript received May 5, 2002; accepted for publication July 15, 2002.

1 Introduction

Compromised delivery of oxygen (O_2) to the tissues of the eye fundus has been implicated in a variety of ocular diseases such as diabetic and other proliferative retinopathies[1–4] and possibly glaucoma.[5] Studies that have investigated the oxygenation of the ocular tissues have been largely performed using O_2-sensitive microelectrodes inserted into the eye to determine the tissue partial pressure ($pO_{2,tissue}$) of O_2 in locally defined regions of the retina[6–10] or the optic nerve head[11–17] (ONH). Except for a limited number of studies investigating the pO_2 in the vitreous of human eyes during ocular surgery,[18–20] this invasive technique has been mainly applied in animals.

The recently developed technique of phosphorescence quenching (PQ) technique by O_2 enables the measurement of the intravascular partial pressure of O_2 in blood ($pO_{2,blood}$) in a noninvasive manner.[21] With PQ, 2-D maps of ONH and retinal $pO_{2,blood}$ were obtained in the eye of cats and piglets at rest and in response to hyperoxia and increased intraocular pressure[22–24] (IOP).

As revealed by recent studies in the brain, transient changes of $pO_{2,blood}$ in the cortex begin less than 1 s after a flash-induced neuronal stimulation and last[25] for less than 10 s. Recent studies suggest that the neural tissues of the ONH may also exhibit such stimulus-induced variations[26,27] of the $pO_{2,blood}$. The 2-D imaging method just mentioned would be too slow, however, to investigate such changes since, at the present time, at least 10 s are needed to acquire the data for calculating a $pO_{2,blood}$ map.[22,23]

With the goal of investigating the transient $pO_{2,blood}$ changes at the ONH in response to various physiological stimuli, we have, therefore, extended the application of the PQ technique to obtain a local measurement of $pO_{2,blood}$ with a time constant of approximately 2.5 s. This measure was also combined with blood flow measurement by laser Doppler flowmetry (LDF).

2 Materials and Methods

2.1 Phosphorescence Quenching by O_2

For *in vivo* measurements of $pO_{2,blood}$, metalloporphyrin molecules capable of phosphorescing are bound to serum albumin before being injected intravenously into the blood stream. A brief flash illuminates the tissue of interest and excites the porphyrin molecules to a triplet state. The excited molecules return to their ground state either through a radiative process (phosphorescence) or by transfer of energy to other molecules (quenching). When measured from a solution containing a large number of quenching molecules, the phosphorescence intensity decays exponentially with a time constant (τ), which represents the time at which the initial intensity is reduced by $1/e$. The only significant quenching agent present in the blood being[28] O_2, τ is related to $pO_{2,blood}$ through the Stern–Volmer equation: $\tau_0/\tau = 1 + k_Q \tau_0 p\mathrm{O}_{2,\mathrm{blood}}$, where τ_0 is the probe lifetime in the absence of a quenching agent, and k_Q the quenching constant.

2.2 Phosphor

The oxygen probe used for PQ measurements is a Pd-meso-tetra (4-carboxyphenyl) porphine (Oxygen Enterprises, Pennsylvania). This compound must be bound to serum albumin before systemic injection. Therefore, blood is drawn from the animal (~4 ml/kg) and the serum is extracted by centrifuga-

Address all correspondence to Stéphane R. Chamot. Tel: (41) 27 203 59 71; Fax: (41) 27 203 59 70; E-mail: stephane.chamot@iro.vsnet.ch

tion at 8000 rpm for 10 min. The probe (20 mg/kg of animal weight) is mixed with the serum, then the pH is adjusted to 7.4, and the serum/probe solution filtered with 0.2-μm sterile filter. The solution is infused intravenously (~100 ml/h) and allowed to equilibrate with the blood before measurements proceed. The binding of the phosphorescent probe to albumin ensures that the parameters τ_0 and k_Q are constant over the range of physiological pH and temperature. The probe's sensitivity to O_2 is also enhanced and its self-quenching is reduced. Since albumin does not diffuse across the wall of the retinal and ONH blood vessels due to the blood retinal barrier, PQ measurements from these tissues provide only data on O_2 dissolved in blood.

In saline solution, the probe absorbs maximally at 412 and 528 nm and its emission spectrum is centered at 706 nm. In the physiological range of pH and blood temperatures (i.e., 7.2 to 7.4 pH unit and 36 to 38 °C, respectively), τ_0 decreases by ~0.8%/°C and ~1% per 0.1 pH unit, whereas k_Q increases by ~3%/°C and ~1% per 0.1 pH unit.[29] Thus, keeping the pH and temperature within the ranges already specified induces a maximum error of ~6% when evaluating $pO_{2,blood}$ based on phosphorescence lifetimes greater than 25 μs ($pO_{2,blood}$ <100 mm Hg). In this study, we used[29] the values of τ_0 and k_Q corresponding to a pH of 7.4 and a temperature of 38 °C (i.e., 637 μs and 381 mm Hg^{-1} s^{-1}, respectively).

2.3 Ocular Fundus Phosphorometer

Figure 1 schematically shows the phosphorometer built to measure $pO_{2,blood}$ in the fundus of the eye. The optics of this device have been mounted on a fundus camera (Zeiss, Germany). To illuminate the fundus with the excitation light, the flash lamp normally supplied for fundus photography was replaced by a flash lamp (F) with shorter pulse width. This unit consisted of a 60-W, 2-μs flash width at half-maximal intensity (Oxygen Enterprises, Ltd., Pennsylvania). An interference filter (IF, XM-530, Corion™, United States; center wavelength = 530 nm, FWMH = 25 nm) placed at the lamp output transmitted the spectral portion of the flash light that matched the absorption spectrum of the phosphorescent probe. Each flash delivered an energy of ~25 μJ/cm^2 over a 30-deg area at the posterior pole. Diffuse illumination of the fundus for alignment or light adaptation of the eye was achieved through the conventional illumination path of the camera starting at the 50-W tungsten lamp (L) and traversing the beamsplitter (BS). The irradiance of the white illumination light measured at the eye fundus was 2 mW/cm^2.

The phosphorescent emission was collected from a localized area ($\varnothing \cong 200$ μm) of the optic disk through the optics used for fundus observation. This area was spatially defined by a pinhole (PH) placed in a retinal image plane of the fundus camera. The phosphorescence was detected by a photomultiplier (PMT) having its maximum sensitivity in the red portion of the spectrum (R928, Hamamatsu, Japan). A long-pass filter (LP, RG630, Schott, Germany) was mounted in front of PH to enhance the phosphorescence detection. Its transmission range was 650 to 800 nm.

The signal at the output of PMT was amplified, then digitized at 1 MHz and fed into an IBM PC compatible computer. Labview (National Instrument, Austin, Texas) software was developed to control the flash triggering, acquire and analyze

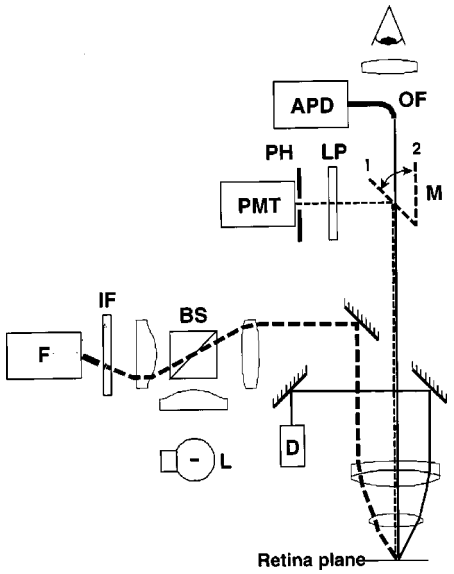

Fig. 1 Zeiss fundus camera modified to incorporate the various optical components necessary for PQ and laser Doppler flowmeter (LDF) measurements: flash source for dye excitation (F), interference filter (IF) for spectral selection of the excitation light, fundus illumination lamp (L), beamsplitter (BS) in the illumination pathway, 670-nm laser diode (D) for LDF measurements, motorized mirror (M) to select PQ or LDF detection pathway (M), long-pass filter (LP) for spectral selection of the phosphorescent light, pinhole (PH) for spatial detection of the phosphorescent light, photomultiplier tube (PMT) for detection of the phosphorescent light, optical fiber (OF) for spatial selection of the laser light, avalanche photodiode (APD) for detection of the laser light.

the phosphorescence data and calculate the $pO_{2,blood}$. To eliminate potentially undesirable contributions to the $pO_{2,blood}$ resulting from the tail of this emission, the recording of the digitized photocurrent started 40 μs after and stopped 2360 μs after triggering the excitation flash. After removing all data points below the dark noise level of the detector, the $pO_{2,blood}$ was obtained based on the average of 10 to 30 successive phosphorescence decay curves obtained at rate of 30 Hz. A linear regression optimized for noise correction (weighted linear fit)[30] was applied to the natural logarithm of all data points to calculate τ and $pO_{2,blood}$, which were then displayed on the Labview stripchart. The total acquisition and computation time for each value of $pO_{2,blood}$ was approximately 2.5 s.

2.4 Blood Flow Measurements

For the quasisimultaneous measurement of blood flow and $pO_{2,blood}$ at the same location of the optic disk, an LDF was incorporated into the phosphorometer. The LDF technique has been previously described in detail.[31] Briefly, a laser beam (670 nm) with long optical coherence is focused on a small area ($\varnothing \cong 150$ μm) of the optic disk, away from the larger vessels. A photomultiplier detects the portion of the laser light scattered by the red blood cells and the surrounding tissue that exits the eye pupil. The photocurrent is amplified, digitized and analyzed by a computer that calculates the relative flow (F_{ONH}) of the red blood cells in the ONH volume sampled by the laser beam.

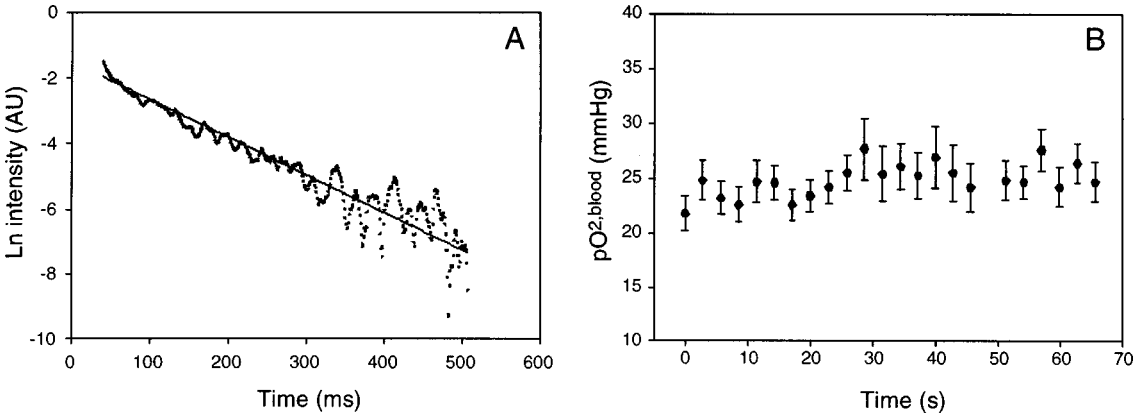

Fig. 2 (a) Typical signal obtained with the phosphorometer by averaging 20 phosphorescence decays; 468 data points above dark noise level were used for analysis. The solid line represents the weighted linear fit of the data logarithm ($R=0.975, p<0.001$), with $\tau=87\pm3$ μs. The $pO_{2,blood}$ calculated by using the Stern–Volmer equation with the appropriate τ_0 and k_Q constant is 26 ± 1 mm Hg. (b) Typical microvascular $pO_{2,blood}$ recording in the ONH achieved a rate of one per 2.5 s.

The LDF system was incorporated into the phosphorometer by having the beam from a visible laser (LDM115, Imatronic, United Kingdom, wavelength=670 nm) follow the optical path of the fundus illumination system of the camera and focusing it precisely at the center of the area from which the phosphorescence was detected. The light scattered by the red blood cells and surrounding tissue in the volume sampled by the laser beam was collected by an optical fiber (OF) placed at the image plane of the illuminated site and guided to an avalanche photodiode (APD). The photocurrent was analyzed using dedicated software running on a NeXT™ computer system to calculate the LDF parameters.[31]

A mirror (M) could be flipped from position 1, which reflected the phosphorescence toward the PH, to position 2 that enabled the scattered laser light to reach the optic fiber. Both PH and OFs were positioned in conjugated retinal image planes and ''looked'' at the same retinal location. Thus, the tip of the optical fiber indicated the location where $pO_{2,blood}$ was measured. The proximity of laser and peak phosphorescence wavelengths did not allow simultaneous LDF and PQ recordings.

2.5 Animals

Experiments were performed on 11 miniature pigs (~10 kg). All procedures conformed to the Association for Research in Vision and Ophthalmology (ARVO) statement for the use of animals in ophthalmic and vision research. After intramuscular injection of a tranquilizer for pigs (Stresnil™, Cilag Chemie AG, Switzerland), anesthesia was induced with 25 to 30 mg of Hypnodil™ (chlorhydrate of metomidate) injected into the ear vein. After arterial and venous catheterization, the pigs were curarized (Tubocurarine™, 1 mg/10 kg), intubated and artificially ventilated. During the experiment, anesthesia was maintained by continuous perfusion of Nabutal™, 4 ml/h, and Tubocurarine™, 0.1 mg/h. The animals were ventilated at approximately 18 strokes/min, with a continuous flow of 20% O_2+80% N_2O using a variable volume respirator (Siemens™ volumeter). The head was secured to avoid movements. Systolic and diastolic blood pressures were monitored via the femoral artery using a transducer (Mingograph™, Siemens-Elema, Switzerland). The systemic arterial pO_2, pCO_2, and pH ($pO_{2,a}$, $pCO_{2,a}$, and pH_a, respectively) were measured intermittently from the same artery with a blood gas analyzer (AVL, automatic gas system 940). Adjustments of ventilatory rate, stroke volume, and the composition of the inspired gas maintained values of $pCO_{2,a}$ of 30 to 35 mm Hg and $pO_{2,a}$ of 100 to 110 mm Hg. A rectal thermometer was used to measure the animal's temperature, which was maintained between 36 and 38°C by means of a thermoblanket with temperature control unit.

2.6 Protocols

All PQ and LDF measurements were performed at a rim location of the optic disk and care was taken to avoid as well as possible the large retinal vessels visible at the disk surface.

In the 11 animals, $pO_{2,blood}$ measurements were collected intermittently during $7:25\pm1:45$ (standard deviation) hours after dye injection at an average of rate of ~5 min^{-1}. Between PQ measurements that were performed in total darkness, the diffuse white fundus illumination (2 mW/cm^2) was occasionally turned on for alignment.

The PQ and LDF techniques were employed alternatively to record the $pO_{2,blood}$ and F_{ONH} response to three different ventilation mixtures, each of which was tested on one animal. After a recording of the baseline $pO_{2,blood}$ and F_{ONH} with the animal ventilated with air (20% O_2+80% N_2O) for approximately 1 min, the breathing conditions were changed. One animal was given 100% N_2O to breathe until death. The second animal received 100% O_2 for 10 min and the third one breathed a CO_2 enriched air mixture (20% O_2+5% CO_2 +75% N_2O) for 12 min. The $pO_{2,blood}$ and F_{ONH} were recorded alternatively.

3 Results

Figure 2(a) shows a typical time course of the logarithm of the phosphorescence intensity and associated linear fit (regression coefficient=0.975, $p<0.001$) to the 810 data points above the dark noise level. The lifetime τ of the phosphorescence was found to be 87 ± 3 μs, a value which, according to the Stern–Volmer equation, corresponds to a $pO_{2,blood}$ of 26

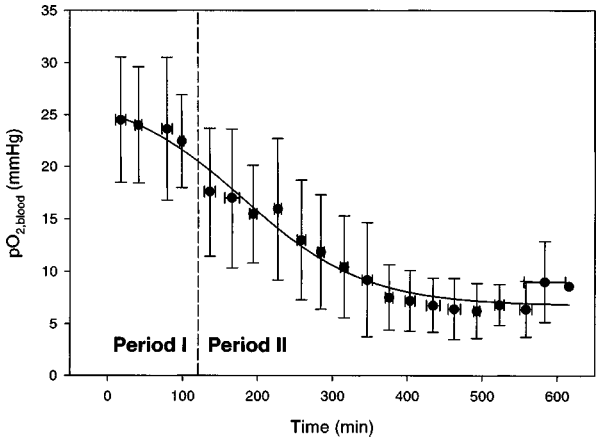

Fig. 3 All the $pO_{2,blood}$ values measured in 11 animals were grouped according to their delay after the phosphor injection (30-min groups). The average value ± standard deviation is plotted here as a function of time. The $pO_{2,blood}$ did not vary significantly [analysis of variance (ANOVA), $p>0.05$] during the first 100 min (period I) but then (period II) dropped significantly (ANOVA; $p<0.001$).

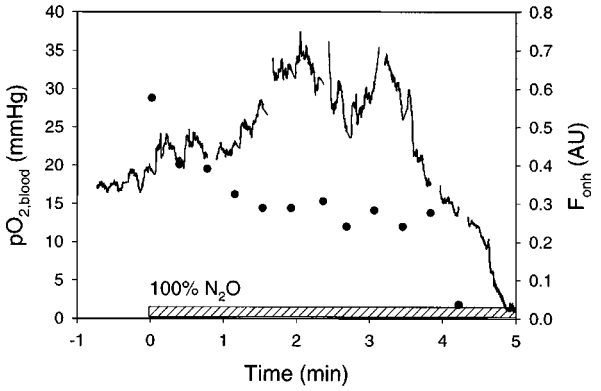

Fig. 4 In one animal, $pO_{2,blood}$ (dots) and F_{ONH} (line) were simultaneously measured at the peripheral ONH during an acute hypoxemia. At time 0, a ventilation with 0% O_2 was used. After 2 min, $pO_{2,blood}$ was decreased by 60% while F_{ONH} increased by 75%.

±1 mm Hg. A typical recording of $pO_{2,blood}$ values obtained with the phosphorometer at a 2.5-s sampling rate is shown in Figure 2(b).

3.1 $pO_{2,blood}$ Time Course

All $pO_{2,blood}$ values collected in the 11 animals were grouped according to the time of their measurement after the phosphor injection (30-min groups). For each group, the mean $pO_{2,blood}$ (± standard deviation) was calculated and plotted versus time (Figure 3). A significant decrease of $pO_{2,blood}$ (ANOVA, $p<0.0001$) was observed, although during the first 120 min of the PQ measurements (period I), the $pO_{2,blood}$ did not change (ANOVA, LSD *post hoc* test, $p>0.05$) and had an average value of 24±1.4 mm Hg. Thereafter (period II), it decreased steadily to a lower level of 7±0.9 mm Hg after 400 min (ANOVA, LSD *post hoc* test, $p<0.05$). In most animals, observations of the eye fundus at this time of the experiment revealed constrictions and even closure of some arteries and veins in the area that had been repeatedly excited for PQ measurements. The retina and ONH tissues were edematous. A breakdown of the blood-retinal barrier was revealed by the leakage of fluorescein observed on angiograms (not shown). In one animal, the contralateral eye, which remained in complete darkness during the 375 min of the PQ investigations on the fellow eye, was prepared for PQ measurements. It appeared entirely normal and $pO_{2,blood}$ averaged over different sites of the disk was 19±2.2 mm Hg. Fluorescein angiography performed on this eye did not show any early or late leakage of the dye.

3.2 Measurements of $pO_{2,blood}$ and F_{ONH}

In the animal that was ventilated with 100% N_2O. The $pO_{2,a}$ dropped continuously, which produced a F_{ONH} increase of 75% and a $pO_{2,blood}$ decrease of 60% (Figure 4).

In the animal ventilated for 10 min with 100% O_2, blood gases taken during normoxia and after 5 min of hyperoxia showed an increase of $pO_{2,a}$ from 109 to 356 mm Hg. Consecutively, a 25% $pO_{2,blood}$ increase and a 23% reduction of F_{ONH} were measured (Figure 5). Both $pO_{2,blood}$ and F_{ONH} returned to baseline levels after the breathing was back to normal.

The animal ventilated with 20% O_2 + 5% CO_2 + 75% N_2O became hypercapnic since the $pCO_{2,a}$ increased from 34.3 to 45.6 mm Hg. Simultaneously, $pO_{2,blood}$ and F_{ONH} increased by 24 and 12%, respectively (Figure 6).

4 Discussion

This paper shows that measurements of $pO_{2,blood}$ and F_{ONH} can be obtained quasisimultaneously at the ONH disk with a fundus camera modified for PQ/LDF. The $pO_{2,blood}$ and F_{ONH} measurements were achieved with a time resolution of 2.5-s (Figure 2) and 47 ms,[31] respectively.

4.1 Range of $pO_{2,blood}$

Several phosphorometers have been developed for studying pO_2 in various biological tissues (muscles, brain, intestine, kidney, tumors).[21,32–37] However, the device presented here is the first that enables focal measurements of $pO_{2,blood}$ in the

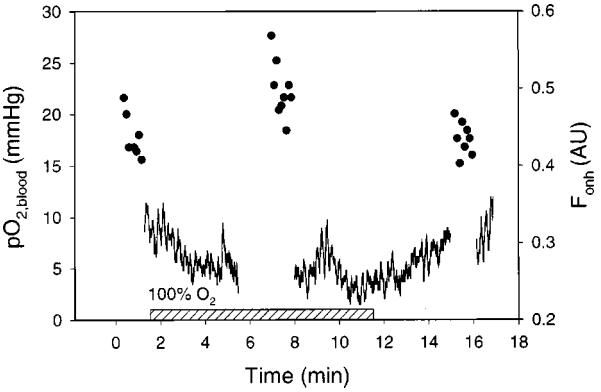

Fig. 5 Recording of $pO_{2,blood}$ (dots) and F_{ONH} (line) at the peripheral ONH during hyperoxia (one animal). After 90 s of baseline, the ventilation was switched to 100% O_2. The F_{ONH} decreased by 22.8% while $pO_{2,blood}$ increased by 25%. The ventilation was switched to normal after 700 s and both parameters went back to their baseline levels.

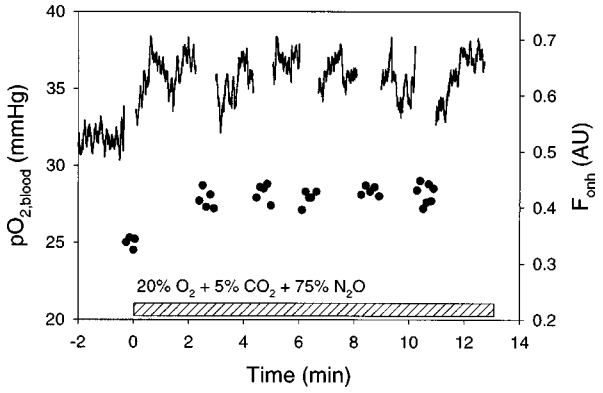

Fig. 6 Recording of $pO_{2,blood}$ (dots) and F_{ONH} (line) at the peripheral ONH during hypercapnia (one animal). After 2 min of baseline, the ventilation was switched to 20% O_2+5% CO_2+75% N_2. The $pO_{2,blood}$ increased by 12% and F_{ONH} by 25%.

ocular fundus. As in the brain, the endothelial cells covering the inner surface of the retinal and ONH vessels in the healthy eye present tight junctions, which prevent the diffusion of soluble molecules such as albumin from the blood into the interstitial tissues (blood-retinal barrier). Therefore, our technique of phosphorescence quenching by O_2 assesses only the phosphorescence emitted by the dye inside the vessels. Values of $pO_{2,blood}$ in the ocular fundus were already measured in pigs and cats with an imaging technique using the phosphorescence quenching principle.[22,24] These studies reported ONH $pO_{2,blood}$ values of 35 ± 9 and 33 mm Hg, respectively, which were higher than those obtained at period I with our phosphorometer in 11 miniature pigs (24 ± 1.4 mm Hg). Even if these two imaging techniques and our phosphorometer applied the same phosphorescence quenching principle, specificity of each instrumental setup or data processing could account for the different $pO_{2,blood}$ range. As pointed out by Golub et al.,[38,39] the temporal characteristic of the flash impulse function influences the shape of the phosphorescence emission (convolution) and consequently its lifetime. Because the excitation light delivered by our instrumental setup reaches its peak intensity after 2 μs, whereas the flash used in these two studies peaked at about 10 μs, the phosphorescence decay emitted by a given tissue sample certainly differs when obtained with different instruments. Furthermore, with the ideal impulse function for time-resolved phosphorescence measurements being a Dirac function, we believe that our $pO_{2,blood}$ measurements obtained with a shorter flash impulse are more accurate than those obtained with flashes of longer duration. Difference in the processing of the phosphorescence emission may also explain the differences between the $pO_{2,blood}$ values obtained with various devices. Whereas Blumenröder et al. used a Levenberg–Marquardt fitting routine for calculating the lifetime of the phosphorescence decay[22] and Shonat et al. a linear fitting routine,[24] we applied a fast, weighted linear fit optimized for noise correction to extract[30] τ. Another important element that has to be considered when comparing the various $pO_{2,blood}$ values is that these were obtained in different species (minipigs, pigs and cats).

As the diffusion of O_2 from the blood vessels into the interstitial ONH tissue depends on (1) the intravascular blood O_2 content, (2) the hemodynamics, (3) the O_2 consumption of the vessel wall, (4) the architecture of the ONH microvascular network, and (5) the metabolic tissue consumption in the ONH, to establish the relation between $pO_{2,tissue}$ and intravascular $pO_{2,blood}$ a diffusion model is required. For the optic nerve, with its complex multilayered vascular systems, such a model is lacking. The $pO_{2,blood}$ values obtained at the ONH in our study are not at odds with $pO_{2,tissue}$ values obtained by others that used O_2-sensitive microelectrodes. Thus, Bouzas et al.[12] found a prepapillary pO_2 of 33.1 ± 3.9 mm Hg at juxta-arteriolar locations and 16.6 ± 1.4 mm Hg at intervascular locations, both with the probe tip positioned at 50 μm in front of the ONH surface. Stefansson et al.,[17] using large microelectrodes with a 100-μm tip, reported an intervascular prepapillary pO_2 of 24.1 ± 11.6 mm Hg. At 50 and 200 μm under the surface of the ONH cup, $pO_{2,tissue}$ was 9.6 ± 1.2 and 9.4 ± 0.8 mm Hg, respectively.[12] At similar depths in the ONH rim, $pO_{2,tissue}$ was[12] 10.8 ± 1.9 and 8.2 ± 1.8 mm Hg. In comparison, $pO_{2,tissue}$ measured between 0- and 200-μm depth into the optic disk of the cat range[11] from 15 to 10 mm Hg. These values measured in the depths of the nerve, compared to the higher values found at the surface of the disc, suggest that our phosphorometer predominantly measures $pO_{2,blood}$ in the retinal layer of the nerve.

4.2 Origin of the Phosphorescence

Due to the topography of the ONH, the depth of tissue sampled with the PQ technique is difficult to evaluate. The green excitation light used for PQ measurements, because of its absorption and scattering by the ONH tissue and blood, should predominantly interact with the dye molecules located in the vessels close to the ONH surface. However, measurements by Koelle et al. using sections of the cat ONH suggest that green light backscattered at a depth of 400 μm from the ONH surface still contributes to the signal detection.[40] In their paper on PQ in the pig, Blumenröder et al.[22] concluded from the fact that the lamina cribrosa cannot be seen by green light ophthalmoscopy that the light does not reach this layer. This argument, however, does not take into consideration that most of the light penetrating the ONH tissue is scattered, a process that may prevent the observation of a clear image of the lamina cribrosa. Regarding the vascular origin of the phosphorescence, placing the pin hole away from the larger vessels at the surface favored detection of phosphorescence from dye circulating in the small arterioles, capillaries, and venules, vessels that are usually not visible with a fundus camera. Therefore, the detected phosphorescence is a superposition of contributions from arterioles, capillaries, and venules. It is expected that, since the venous blood volume exceeds the arterial and capillary blood volumes, the major contribution of the measured $pO_{2,blood}$ comes from venules. This contribution is further emphasized by the fact that quenching is weaker for the vessels with low $pO_{2,blood}$ than for those with high $pO_{2,blood}$.

4.3 Time Course of $pO_{2,blood}$ during Prolonged PQ Measurements

The decrease of $pO_{2,blood}$ during the period II of the PQ measurements is probably due to a decreased blood flow, as suggested by the marked constriction of the vasculature and

white appearance of the ONH tissue in the region illuminated by the excitation light that was observed toward the end of this period. As the maximum irradiance used for each $pO_{2,blood}$ measurements (30 flashes$\times 25\ \mu J/cm^2 = 750\ \mu J/cm^2$ at 530 nm) is below the maximum permissible ocular exposure[41] for a continuous exposure of 1 s (30 flashes delivered at 30 Hz), the damage observed at the ocular fundus is not the consequence of a thermic process, but likely results from the photoactivation of our phosphor. Light activation of intravascularly administered fluorochromes is known to generate toxic oxygen species, including singlet oxygen and superoxide anions. Various deleterious microvascular effects such as platelet thrombus formation, arteriolar constriction, or postcapillary venular leakage have been reported and attributed to the luminal generation of oxidant species.[42] These effects provide the basis of the photodynamic treatment of tumors.[43] As the quenching of an activated phosphor by an O_2 molecule also produces a singlet oxygen molecule, extended $pO_{2,blood}$ measurements with the phosphorescence quenching technique may lead to vascular damage.

In one animal, the contralateral eye was also investigated at period II (direct observation, $pO_{2,blood}$ measurements, fluorescein angiography). In this eye, which remained in darkness for hours before, the ocular fundus looked normal and $pO_{2,blood}$ was approximately 19 mm Hg. It shows that the porphyrin dye, if not optically excited, does not affect the $pO_{2,blood}$ level, which supports the preceeding hypothesis on alterations due to photoactivation of the phosphorescent probe.

In our system, two sources of phosphorescence excitation susceptible to induce photoactivation were present. One was the flash for excitation of the dye, the other the white light used for fundus observation. According to the data of Shonat et al.,[33,35] the energy density delivered to obtain a $pO_{2,blood}$ measurement ($\sim$750 mJ/cm^2) should not affect the tissue. We presume that it is the visible light used to occasionally observe the fundus that caused the most severe photoactivation and produced tissue alterations resulting in the drop of the $pO_{2,blood}$ in period II.

Future studies will benefit from any attempt to reduce the likelihood of alterations due to photoactivation, such as improving the phosphorescence detection sensitivity and reducing the number of flashes needed for the average phosphorescence decay curve, decreasing the dye concentration and removing the spectral component of the observation light likely to induce photoactivation.

4.4 Modification of the Ventilation Conditions

Previous PQ or LDF measurements at the ONH during hypoxemia reported that $pO_{2,blood}$ drops,[22] and F_{ONH} increases[44] by 67 to 89%. Our measurement, albeit in only one animal, is in agreement with these results. It also illustrates the feasibility of quasisimultaneous measurements at the ONH rim of $pO_{2,blood}$ and F_{ONH}, since 100% N_2O breathing induced a 60% decrease and a 75% increase of these parameters, respectively. This measurement illustrates the regulation capabilities of the ONH vasculature, which compensates the drop of the arterial blood O_2 content by increasing blood flow.

LDF measurements performed during hyperoxia (100% O_2 breathing) showed blood flow decreases of 39 to 49% in cats[44] and 25% to 38% in humans.[45,46] Using the PQ imaging technique, $pO_{2,blood}$ was also measured at the optic disc during hyperoxia in 6 piglets.[22] In that study, $pO_{2,blood}$ rose from 35 ± 9 to 44$\pm$ 14 mm Hg, while $pO_{2,a}$ was increased from 100 to 120 mm Hg with an O_2-rich ventilation. Our measurement during hyperoxia (100% O_2 breathing) shows that $pO_{2,blood}$ increased by 25%, whereas $pO_{2,a}$ raised by 226%. The difference between the increase of $pO_{2,a}$ and $pO_{2,blood}$ indicates a regulation mechanism that prevents excessive amounts of O_2 to reach the ocular microcirculation.

CO_2 has a vasodilating effect on the blood vessels, which can enhance the blood perfusion. Our F_{ONH} measurement is in accordance with a study by Harris,[46] who reported a similar 28% increase of the ONH blood flow when using the same gas mixture. A higher perfusion apparently contributes to increase the supply of O_2 to the capillaries since $pO_{2,blood}$ increased by approximately 12%.

The good agreement of the results obtained during hypoxemia, hyperoxia, and hypercapnia with the literature shows that $pO_{2,blood}$ and blood flow measurements can be reliably measured quasisimultaneously in the microcirculation of the prelaminar optic nerve. This instrument is specifically adapted for investigating with a good time resolution the time course of transient $pO_{2,blood}$ changes that could occur during various physiological perturbations.

Acknowledgments

The authors wish to thank Jean-Luc Munoz for the preparation of the animals. This work was supported in part by Grant No. 3100-057045 and 3200-61685 from the Swiss National Foundation for Scientific Research and a grant from the Loterie Romande.

References

1. P. A. D'Amore, ''Mechanisms of retinal and choroidal neovascularization,'' *Invest. Ophthalmol. Visual Sci.* **35**(12), 3974–3979 (1994).
2. C. J. Pournaras, ''Retinal oxygen distribution. Its role in the physiopathology of vasoproliferative microangiopathies,'' *Retina* **15**(4), 332–347 (1995).
3. E. Stefansson, M. B. Landers III, and M. L. Wolbarsht, ''Oxygenation and vasodilatation in relation to diabetic and other proliferative retinopathies,'' *Ophthalmic Surg.* **14**(3), 209–226 (1983).
4. G. N. Wise, ''Retinal neovascularization,'' *Trans. Am. Ophthalmol. Soc.* **54**(729), 826–835 (1956).
5. S. S. Hayreh, ''The pathogenesis of optic nerve lesions in glaucoma,'' *Trans. Am. Acad. Ophthalmol. Otolaryngol.* **81**(2), 197–213 (1976).
6. V. A. Alder and S. J. Cringle, ''Vitreal and retinal oxygenation,'' *Graefe's Arch. Clin. Exp. Ophthalmol.* **228**, 151–157 (1990).
7. R. A. Linsenmeier, ''Effects of light and darkness on oxygen distribution and consumption in the cat retina,'' *J. Gen. Physiol.* **88**, 521–542 (1986).
8. C. E. Riva, C. J. Pournaras, and M. Tsacopoulos, ''Regulation of local oxygen tension and blood flow in the inner retina during hyperoxia,'' *J. Appl. Physiol.* **61**(2), 592–598 (1986).
9. J. Ahmed, R. D. Braun, R. Dunn, Jr., and R. A. Linsenmeier, ''Oxygen distribution in the macaque retina,'' *Invest. Ophthalmol. Visual Sci.* **34**(3), 516–521 (1993).
10. S. J. Cringle, D. Y. Yu, V. A. Alder, and E. N. Su, ''Oxygen tension and blood flow in the retina of normal and diabetic rats,'' in *Oxygen Transport to Tissue XIV*, W. Erdmaann and D. F. Bruley, Eds., pp. 787–791, Plenum, New York (1992).
11. J. Ahmed, R. A. Linsenmeier, and R. Dunn, ''The oxygen distribution in the prelaminar optic nerve head of the cat,'' *Exp. Eye Res.* **59**, 457–466 (1994).
12. E. A. Bouzas, G. Donati, and C. J. Pournaras, ''Distribution and regulation of the optic nerve head tissue PO_2,'' *Surv. Ophthalmol.* **42**(2), 1–8 (1997).
13. D. G. Buerk, D. N. Atochin, and C. E. Riva, ''Simultaneous tissue

pO_2, nitric oxide, and laser Doppler blood flow measurements during neuronal activation of optic nerve head," in *Oxygen Transport to Tissue XX*, A. Hudetz and D. F. Bruley, Eds., pp. 159–164, Plenum, New York (1998).
14. J. T. Ernest, "Autoregulation of optic-disc oxygen tension," *Invest. Ophthalmol.* **13**(2), 101–106 (1974).
15. J. T. Ernest, "Optic disc oxygen tension," *Exp. Eye Res.* **24**, 271–278 (1977).
16. C. E. Riva, C. J. Pournaras, C. L. Poitry-Yamate, and B. L. Petrig, "Rhythmic changes in velocity, volume, and flow of blood in the optic nerve head tissue," *Microvasc. Res.* **40**(1), 36–45 (1990).
17. E. Stefansson, P. K. Jensen, T. Eysteinsson, K. Bang, J. F. Kiilgaard, J. Dollerup, E. Scherfig, and M. la Cour, "Optic nerve oxygen tension in pigs and the effect of carbonic anhydrase inhibitors," *Invest. Ophthalmol. Visual Sci.* **40**, 2756–2762 (1999).
18. H. Sakaue, Y. Tsukahara, A. Negi, N. Ogino, and Y. Honda, "Measurement of vitreous oxygen tension in human eyes," *Jpn. J. Ophthalmol.* **33**(2), 199–203 (1989).
19. H. Sakaue, A. Negi, and Y. Honda, "Comparative study of vitreous oxygen tension in human and rabbit eyes," *Invest. Ophthalmol. Visual Sci.* **30**(9), 1933–1937 (1989).
20. E. Stefansson, R. Machemer, E. de Juan, Jr., B. W. McCuen, and J. Peterson, "Retinal oxygenation and laser treatment in patients with diabetic retinopathy," *Am. J. Ophthalmol.* **113**(1), 36–38 (1992).
21. J. M. Vanderkooi, G. Maniara, T. J. Green, and D. F. Wilson, "An optical method for measurement of dioxygen concentration based upon quenching of phosphorescence," *J. Biol. Chem.* **262**(12), 5476–5482 (1987).
22. S. Blumenröder, A. J. Augustin, and F. H. J. Koch, "The influence of intraocular pressure and systemic oxygen tension on the intravascular pO_2 of the pig retina as measured with phosphorescence imaging," *Surv. Ophthalmol.* **42**(1), S118–S126 (1997).
23. R. D. Shonat, D. F. Wilson, C. E. Riva, and S. D. Cranstoun, "Effect of acute increases in intraocular pressure on intravascular optic nerve oxygen tension in cats," *Invest. Ophthalmol. Visual Sci.* **33**(11), 3174–3180 (1992).
24. R. D. Shonat, D. F. Wilson, C. E. Riva, and M. Pawlowski, "Oxygen distribution in the retinal and choroidal vessels of the cat as measured by a new phosphorescence imaging method," *Appl. Opt.* **31**(19), 3711–3718 (1992).
25. D. Malonek, U. Dirnagl, U. Lindauer, K. Yamada, I. Kanno, and A. Grinvald, "Vascular imprints of neuronal activity: Relationships between the dynamics of cortical blood flow, oxygenation, and volume changes following sensory stimulation," *Proc. Natl. Acad. Sci. U.S.A.* **94**, 14826–14831 (1997).
26. D. G. Buerk, C. E. Riva, and S. D. Cranstoun, "Frequency and luminance-dependent blood flow and K^+ ion changes during flicker stimuli in cat optic nerve head," *Invest. Ophthalmol. Visual Sci.* **36**, 2216–2227 (1995).
27. C. E. Riva and D. G. Buerk, "Dynamic coupling of blood flow to function and metabolism in the optic nerve head," *J. Neuroophthalmol.* **20**(2), 45–54 (1998).
28. D. F. Wilson, A. Pastuszko, J. E. DiGiacomo, M. Pawlowski, R. Schneiderman, and M. Delivoria-Papadopoulos, "Effect of hyperventilation on oxygenation of the brain cortex of newborn piglets," *J. Appl. Physiol.* **70**(6), 2691–2696 (1991).
29. L.-W. Lo, C. J. Koch, and D. F. Wilson, "Calibration of oxygen-dependent quenching of the phosphorescence of Pd-meso-tetra (4-carboxyphenyl) porphine: a phosphor with general application for measuring oxygen concentration in biological systems," *Anal. Biochem.* **236**, 153–160 (1996).
30. W. H. Press, B. P. Flannery, S. A. Teukolsky, and W. T. Vetterling, in *Numerical Recipes in C: The Art of Scientific Computing*, pp. 523–528, Cambridge University Press, Cambridge (1988).
31. B. L. Petrig and C. E. Riva, "Optic nerve head laser Doppler flowmetry: principles and computer analysis," in *Ocular Blood Flow*, H. J. Kaiser, J. Flammer, and P. Hendrickson, Eds., pp. 120–127, Karger, Basel (1996).
32. T. J. Green, D. F. Wilson, J. M. Vanderkooi, and S. P. DeFeo, "Phosphorimeters for analysis of decay profiles and real time monitoring of exponential decay and oxygen concentrations," *Anal. Biochem.* **174**(1), 73–79 (1988).
33. R. D. Shonat, K. N. Richmond, and P. C. Johnson, "Phosphorescence quenching and the microcirculation: an automated, multipoint oxygen tension measuring instrument," *Rev. Sci. Instrum.* **66**(10), 5075–5084 (1995).
34. L. Zheng, A. S. Golub, and R. N. Pittman, "Determination of pO_2 and its heterogeneity in single capillaries," *Am. J. Physiol.* **271**(40), H365–H372 (1996).
35. R. D. Shonat, E. S. Wachman, W. Niu, A. P. Koretsky, and D. L. Farkas, "Near-simultaneous hemoglobin saturation and oxygen tension maps in mouse brain using AOTF microscope," *Biophys. J.* **73**, 1223–1231 (1997).
36. F. Torres, I. and M. Intaglietta, "Microvessel PO_2 measurements by phosphorescence decay method," *Am. J. Physiol.* **265**(4, Pt. 2), H1434–H1438 (1993).
37. M. Sinaasappel, C. Donkersloot, J. van Bommel, and C. Ince, "PO_2 measurements in the rat intestinal microcirculation," *Am. J. Physiol.* **276**(6, Pt. 1), G1515–G1520 (1999).
38. A. S. Golub, A. S. Popel, L. Zheng, and R. N. Pittman, "Analysis of phosphorescence decay for nonuniform oxygen tension. Consequences of finite excitation flash duration," *Adv. Exp. Med. Biol.* **471**, 649–659 (1999).
39. A. S. Golub, A. S. Popel, L. Zheng, and R. N. Pittman, "Analysis of phosphorescence decay in heterogeneous systems: consequences of finite excitation flash duration," *Photochem. Photobiol.* **69**(6), 624–632 (1999).
40. J. S. Koelle, C. E. Riva, B. L. Petrig, and S. D. Cranstoun, "Depth of tissue sampling in the optic nerve head using laser Doppler flowmetry," *Laser Med. Sci.* **8**, 49–54 (1993).
41. *American National Standard for Safe Use of Lasers*, p. 85, Laser Institute of America, Orlando (2000).
42. V. H. Fingar, "Vascular effects of photodynamic therapy," *J. Clin. Laser Med. Surg.* **14**(5), 323–328 (1996).
43. T. J. Wieman and V. H. Fingar, "Photodynamic therapy," *Surg. Clin. North Am.* **72**(3), 609–622 (1992).
44. C. E. Riva, S. Harino, B. L. Petrig, and R. D. Shonat, "Laser Doppler flowmetry in the optic nerve," *Exp. Eye Res.* **55**, 499–506 (1992).
45. A. Lietz, P. Hendrickson, J. Flammer, S. Orgül, and I. O. Haefliger, "Effect of carbogen, oxygen and intraocular pressure on Heidelberg retina flowmeter parameter "flow" measured at the papilla," *Ophthalmologica* **212**, 149–152 (1998).
46. A. Harris, "Laser Doppler flowmetry measurement of changes in human optic nerve head blood flow in response to blood gas perturbations," *J. Glaucoma* **5**, 258–265 (1996).